Coupling economic multi-objective optimization and multiple design options: A business-oriented approach to size an off-grid hybrid microgrid

Article *in* International Journal of Electrical Power & Energy Systems · May 2021

DOI: 10.1016/j.ijepes.2020.106686

5 authors, including:

Davide Fioriti
Università di Pisa
49 PUBLICATIONS 303 CITATIONS

Giovanni Lutzemberger
Università di Pisa
98 PUBLICATIONS 985 CITATIONS

D. Poli
Università di Pisa
105 PUBLICATIONS 1,411 CITATIONS

Andrea Micangeli
Sapienza University of Rome
64 PUBLICATIONS 577 CITATIONS

Coupling economic multi-objective optimization and multiple design options: a business-oriented approach to optimize an off-grid hybrid microgrid

Davide Fioriti[a,*], Giovanni Lutzemberger[a], Davide Poli[a], Pablo Duenas-Martinez[b], Andrea Micangeli[c]

[a] *DESTEC, University of Pisa, Largo Lucio Lazzarino, 56122 Pisa, Italy*
[b] *MIT Energy Initiative, Massachusetts Institute of Technology, 77 Massachusetts Avenue, 02139, Cambridge, MA, United States*
[c] *DIMA, "Sapienza" University of Rome, Piazzale Aldo Moro, 5, 00185 Rome, Italy*

Abstract

Achieving the maximum economic profitability is a priority for microgrid developers. However, although economic indicators usually dominate the business decision making, rarely numerical indicators are fully able to capture the entire sociopolitical, technical and geographical circumstances affecting the business environment, especially in rural areas of developing countries. Typical planning approaches achieve a single solution, or a set of solutions in multi-objective approaches, and near-optimal solutions are usually discarded even when they may better fit the specific multi-faceted circumstances of a project. In this paper, we propose a multi-objective approach that not only calculates the traditional Pareto-frontier but also compiles near-optimal solutions that enlarge the options portfolio for microgrid developers. The proposed iterative approach stores all the simulated solutions, and post-processes them to provide the developer with multiple design options (MDO). A numerical case study of a Kenyan hybrid microgrid using real data confirms that near-optimal solutions can correspond to extremely different design solutions, even ±100% w.r.t. the Pareto-efficient ones, with only very limited disparities in the economic objective functions. The results, supported by a Key Performance Indicator (KPI) analysis, show that MDO methodology can successfully support the business decision making and help developers size microgrids considering several nearly-equivalent sizing options.

Keywords: Multiple Design Options (MDO); multiple sizing choices; solution pool; hybrid energy system; mini-grid; Multi-Objective Particle Swarm Optimization (MDO-MOPSO)

---

*Corresponding author

Email addresses: davide.fioriti@ing.unipi.it (Davide Fioriti), pduenas@mit.edu (Pablo Duenas-Martinez), andrea.micangeli@uniroma1.it (Andrea Micangeli)

Nomenclature

Acronyms

NPC Net Present Cost

CAPEX Investment costs

OPEX Operating expenses

REP/RES Replacement costs and residual value of the assets

MILP Mixed-Integer Linear Programming

MOPSO Multi-Objective Particle Swarm Optimization

MDO Multiple Design Option

DMS Direct Multi Search

NSGA Non-dominated Sorting Genetic Algorithm

LFS Load Following Strategy

ENS Energy Not Served

PV Photovoltaic

KPI Key Performance Indicator

Indices and sets

$t \in T$ Index and set of the time steps

$y \in Y$ Index and set of the years of the microgrid project

$i \in I$ Index and set of piece-wise linear formulation to model fuel costs

$a \in A$ Index and set of the assets of the microgrid (D: generator; C: battery converter; I: inverter; B: battery; RAC/RDC: renewable source at the AC or DC busbar)

S^{PF} Set of points belonging to the Pareto frontier within the search area

S^{MDO} Set of MDOs selected by the proposed procedure in the search area

Variables and expressions

NPC Net Present Cost

$CAPEX$ Investment costs

$OPEX_y$ Operating charges

REP_y/RES_y Replacement costs and residual value

$C_y^{a,M}$ Yarly operating and maintenance charges of asset a, excluding the fuel generator

C_t^D Fuel costs of the fuel generator

$C_t^{D,M}$ Maintenance costs of the fuel generator

C_t^{LC} Load curtailment charges

X^a Installed capacity for each technology a

P_t^D Dispatch of the fuel generator

$P_t^{I+/-}$ Dispatch of the inverter

$P_t^{B+/-}$ Dispatch of the battery

$P_t^{RAC/RDC}$ Dispatch of the renewable assets at the AC/DC busbar

P_t^L Load

$DI^{A/N}(P); DI^{A/N}(P,Q)$ Absolute (A) or Normalized (N) diversity index of the points belonging to set P or to the points between set P and Q

Z_t^D Unit commitment of the fuel-fired generator

Parameters

d Discount factor

$c_0^a; x_0^a; \beta^a$ Parameters to describe the economies of scale and volume of asset a

$\alpha^{D,min}$ Minimum working point of the fuel generator

$\alpha^{B,min/max}$ Minimum and maximum level of the battery storage

$p_t^{RAC/RDC}$ Specifid renewable production for installed capacity for AC and DC renewable assets

$\eta^{B/I}$ Efficiency of the battery system (round-trip) and of the inverter

π^F Fuel costs

c^{LC} Load curtailment charges

$c_i^{D,I}; c_i^{D,S}$ Intercept and slope modelling the piece-wise linear consumption of the fuel generator

1. Introduction

1.1. Motivation

The business environment of microgrid developers is known to be very complex and multi-faceted due to the local sociopolitical and geographical framework the technical solution must comply with. This is particularly challenging in off-grid systems both of developed and developing countries, where the revenue stream can be difficult to predict due to the uncertain load demand, the precarious continuity of supply and the possible curtailment of exceeding renewable production [1]. In this contexts, the optimal sizing of a system cannot but include non-technical concerns and rarely mathematical formulation are fully able to capture all the drivers and circumstances of the project.

Multiple-decision making has been widely used to tackle this issue [2], fed by multi-objective optimization that is able to capture the trade-off between different numerical indicators/targets [3] and identify the set of solutions that correspond to non-dominated values of the objective functions [4, 5, 3, 6], where a point A "dominates" a solution B when all the objective functions in A are better or equal than those in B. However, these approaches are objective-centric and they usually disregard possible multiple designs that can lead to the same point of the Pareto frontier, as noticed in [7] for a single-objective approach.

In this paper we focus on developing a methodology able to capture multiple design options that can lead to values as profitable as the points of the Pareto frontier, so to enhance the design capabilities of microgrid developers.

1.2. Literature review

The business decision making of microgrid developers is typically focused on economic indicators [8, 9, 10, 11, 12], as private companies are mostly concerned about making economic profits. However, reliability [13, 9, 12], environmental [14, 10, 12], technical [15, 12] or socio-political [11, 12] aspects have been increasingly taken into consideration in the decision process, due to policy obligations, environmental constraints, visibility, among other reasons [12, 16, 17]. Moreover, even when only economic concerns are considered, different indicators may lead to completely different optimal designs of the system and mislead the developer [18]; this is why the authors in [18] recommended to use at least two economic indicators for business projects. Moreover, due to the intrinsic complexities and lack of data, rarely the mathematical modeling is able to capture all circumstances involved in the optimal sizing of a microgrid, such as availability of local skills, logistics of the supply chain [7], especially in the difficult conditions of developing countries [19]. Therefore, according to their expertise and eventually supported by multi-criteria decision tools [3], developers often prefer to choose the optimal solution among a set of possible options and multi-objective optimization is the most appropriate tool, which is enhanced in this paper to provide additional support for the decision making. In particular, as rarely combined in the literature of multi-objective optimization [18], we considered two main economic objective functions: Net Present Cost and CAPEX.

As reviewed in [20, 21, 12, 6, 3], the literature on multi-objective optimization for hybrid microgrids is rich and typically all methodologies focus on identifying the Pareto frontier. However, in [7], the authors first introduced the concept of "Multiple Design Options" (MDO) and proved that different size configurations can achieve similar levels of profitability, yet in a single-objective environment. In particular, the MDO set is a group of configurations, whose objective function is within a given tolerance from the optimal value [7]. This methodology, based on Particle Swarm Optimization, iteratively simulates and stored all the intermediate results of the algorithm to be later analyzed by means of basic plots. The novel idea of this approach is that partially sub-optimal design, which exhibit only a slight worse profitability, but possibly a significantly different size of components, might be more suitable for a specific project, given some characteristics that can be easily addressed by the human developer but that are hard to model in mathematical solvers. In fact, non-technical aspects, such as community engagement, local awareness, political stability, local skills, supply chain uncertainties, acceptance of the technology, among others [22, 23, 1], play a paramount role in the success of microgrid projects [24], but they are difficult to be modelled and quantified. To clarify, let's suppose that a fully wind-diesel configuration (A) is selected as optimal by the solver and let's suppose that another PV-diesel configuration (B) is only 0.1% more expensive than A. In this case, the solver would return A as optimal and discard B; however, the developer would be willing to receive both results to evaluate if the lower maintenance complexity and uncertainty of the PV configuration is more suitable for the investment, also given the labor skills of the population nearby the site of the project. In this case, configuration B would belong to the MDO set. To the best of the authors' knowledge, MDO has been discussed only in [7], where the authors highlighted that different size configurations can lead to similar values of the objective function in a single-objective environment by using charts, so that operators shall select the final solution with a manual procedure, as done also in [25, 26]. However, such approach focused on a single-objective and was limited to displaying plots without providing a limited number of options best suited for the developer. Therefore, that approach can be performed only with simple configurations and with a limited number of objectives; otherwise the developer may be unable to manage the corresponding complexities. To the best of the authors knowledge supported by the literature review [21, 12, 6, 3], no other paper has proposed an integrated framework to to extend the concept of MDO to multi-objective approaches, and here we propose to extend the definition of MDO in a multi-objective environment.

On the algorithmic perspective, the state-of-the-art on multi-objective optimization is dominated by (meta-)heuristic methodologies [6, 3], given their ability to handle complex systems [27, 28, 29]. Mathematical programming, such as Mixed-Integer Linear Programming (MILP), has been also proposed, but it usually requires longer computational time and relevant simplifications, especially when the problem is non-linear, to moderate the computational burden [30, 31], given the intrinsic limitations in the mathematical formulation [32]. Moreover, according to the study in [33] on home-system management, the heuristic formulation of the problem required only 10% of the time of the MILP procedure, with negligible differences in terms of results. In design approaches where the size of the problem is larger, the computational requirements of heuristic problems can be as low as 3% the performances of MILP with equal optimality of the results [34]. Therefore, a meta-heuristic formulation has been considered in this study.

Several heuristic methodologies have been proposed for different system models, however, according to our analysis, no other paper has ever discussed MDO in a multi-objective perspective [6, 20]. The authors in [29] proposed a multi-objective analysis based on heuristic methodologies for a hybrid PV-battery-diesel microgrid in the Gobi Desert and the multi-objective problem is modeled as a single-objective problem using ϵ-constraint and Particle Swarm Optimization method, accounting for emissions, NPC and system reliability. The authors confirmed that PSO performs better than genetic algorithm or simulated annealing. The study in [14] went beyond and addressed the possible installation of distributed PV-battery systems in an off-grid system so to reduce the levelized cost of electricity and emissions, and increase voltage grid quality, using Non-dominated Sorting Genetic Algorithm (NSGA); however, no comparison with the centralized approach is described. The multiple objective version of PSO has been developed in [35] and successfully applied to various systems [36, 37, 38, 39]. PV-wind-hydro [36], PV-wind-battery-diesel [37, 40], microgrids both with reliability and economic objectives have been successfully addressed by Multi-Objective Particle Swarm Optimization (MOPSO); such studies highlighted high capabilities of MOPSO to handle large population of points. MOPSO has also been used for the co-joint planning of wind farms and PV systems in large farms [41] or the optimal unit commitment subject to uncertainties [42]; for these reasons, it is regarded as a flexible tool easily able to handle different systems configurations. The results of the study in [38] confirmed MOPSO to achieve a better Pareto frontier than NSGA, except at the extrema; in [43], MOPSO performed better than all the other multi-objective methodologies under consideration. Other multi-objective methodologies refer to Direct Multi-Search (DMS) [18], a modified version of the Cuckoo Search or Artificial Bee Colony Algorithm [44]; however, given its simplicity, its ability to easily handle large numbers of the Pareto frontier and its good convergence performance, MOPSO has been used in our activity.

In the case of off-grid systems, the system management is traditionally performed by using simple priority-list criteria, such as the Load Following Strategy (LFS) [45, 14, 40]. According to LFS, renewable sources are prioritized and batteries are dispatched to keep the system stable; the fuel-fired generator is turned on only when the other components cannot meet the demand. More advanced predictive approaches have also proved to reduce the operating costs even by 8% [34], given the same sizing [34]; however, in terms of Net Present Costs, the savings with respect to LFS are much more limited (<1-3%) [34, 18]. Similar findings are also supported by [46], in which the cost reduction enabled by predictive scheduling is usually below 3%, except for very large systems in which savings can scale up to 6%. However, while priority-list approaches require limited computational requirements (few minutes), the calculation times of predictive methodologies are significantly larger (even hours) [34]. In rural microgrids that are characterized by large uncertainties in forecasting the social behavior of the community, lack of connectivity, and limited assets, robust dispatching methodologies are required and usually priority-list approaches are preferred, so they constitute the state-of-the-art for newly developed systems. Anyway, as the load grows, forecasting its power profile becomes easier, so predictive methodologies are worth considering. The study in [34] pointed out that optimal sizing should be performed by simulating the actual system operation, otherwise costs could increase even by 15%. Given the limited benefits in terms of results, the generality of the approach, the limited differences between predictive and non-predictive methodologies, and the current state-of-the-art of rural microgrids, in this activity we simulated the realistic operation of a rural microgrid based on Load Following Strategy.

According to the proposed literature review, no other paper has addressed the concept of MDO for multi-objective optimization and in this activity we show the benefits of MDO for an off-grid system in developing country, which represents a very multifaceted challenge that microgrid developers are facing.

1.3. Contributions

In this paper we develop a multi-objective approach that compiles multiple design options (MDO) to provide the developers with additional design criteria that go beyond the traditional Pareto frontier. For the purpose of this activity, we aspired to improve the preliminary single-objective MDO approach proposed in [7], so we define MDO as a selected set of points with different design characteristics within a given optimality tolerance from the Pareto frontier. MDOs are selected thanks to a modified MOPSO algorithm, in which all intermediate simulated points are stored and post-processed after the convergence of the methodology. The post-processing phase identifies the final MDO points as those maximizing selected performance indicators, which are also compared to the traditional Pareto frontier by means of Key Performance Indicators (KPI), to support the robustness of our approach. Moreover, a correlation analysis highlights the trade-off among the size configurations of the components nearby the Pareto front and supports the planning phase of developers. A sensitivity analysis is performed on the optimality tolerance to highlight how the size of the selected points changes. A numerical case study is performed for the case of a rural PV-Wind-Battery-Diesel microgrid in Kenya.

In short, the main novelties of the paper can be listed as follows.

- Extension of the MDO concept to multi-objective optimization.
- Development of a custom MDO-MOPSO algorithm and a post-processing procedure to select the MDO points that maximize energy indicators (maximum PV/wind penetration, minimum ENS, etc.).
- Application of MDO to a multi-source hybrid system, including PV, wind, battery and fuel-fired generation.

- Correlation analysis to highlight and quantify the relationship among the optimal size of the assets with very similar level of profitability.

- Definition of Key Performance Indicators to compare the proposed enhanced MDO set of solutions and the traditional Pareto frontier.

Section II shows the microgrid model. Section III discusses the proposed MDO multi-objective procedure. Section IV and V describe respectively the case study and the results. Finally, conclusions are drawn.

2. The system model

2.1. Description

Given the sensitive characteristics of the investment and without loss of generality, in this activity we consider the case of a typical off-grid system in developing countries, composed by renewable energy and storage units, and a backup fuel-fired generator. The photovoltaic plant and batteries are coupled to a DC busbar, while the fuel-fired generator, while other renewable sources (i.e. wind or hydro) and the inverter are tied at the AC busbar and directly supply the load, as shown in Fig. 1. The inverter is considered to be grid-forming so that it can contribute to the system stability, according to the power and energy limits of the battery and the PV system. The proposed model, whose mathematical representation is based on [18, 14, 36], is aimed to best capture the main characteristics of a microgrid project in developing countries for sizing purposes, so to build a robust framework to discuss and apply the MDO methodology.

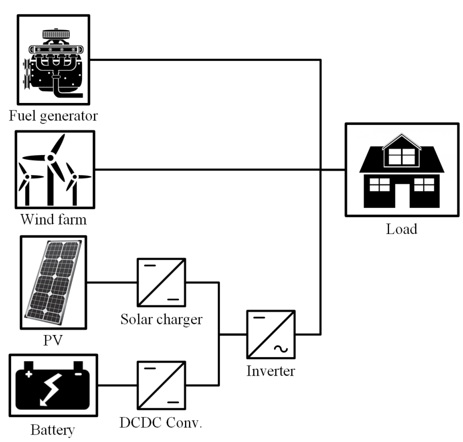

Figure 1: Schematics of the microgrid.

2.2. Operating strategy

A control system is assumed to coordinate the energy flows and to minimize the operating costs. Although predictive methodologies have been proposed for microgrid operation in developing countries [18], the demand forecasting can be significant uncertain and jeopardize the benefits of complex approaches. Due to its simplicity, limited hardware requirements and negligible communication needs, typical rural microgrids are then usually operated by simple operating rules based on priority-list criteria: all sources are dispatched according to "if-then" rules and a merit-order list that typically first exploits the renewable energies, then batteries and finally the fuel-fired generators [18]. The most common strategy is the so-called "Load Following Strategy" (LFS), under which the fossil-fuel generator is turned on only to supply the load when the other components cannot. The generator is shut down when batteries and the other devices are able to keep the system balanced. For these reasons and to represent a realistic rural system for developing countries, a LFS has been considered in this paper.

2.3. Mathematical model

The simulations of the microgrid operation have been developed on the basis of the activity reported in [18] but now expanded to include additional components, such as wind turbines. Technical and physical constraints of the system are considered, whose equations are reported below.

The main economical functions considered in this study are Net Present Cost (NPC) and investment costs (CAPEX), which are well known in the literature and of major interest for developers. The mathematical formulation of NPC, shown in (1), accounts for $CAPEX$, operating costs $OPEX_y$ of the system in year y, replacement costs REP_y of the assets due to aging, and the residual value of the assets at the end of the project, RES_y. The detailed model of CAPEX, shown in (2), accounts for the economy of scale and volume of each asset a. CAPEX are modelled with an exponential function in which C_0^a is the reference cost corresponding to a component of capacity x_0^a; β^a, instead, models the economies of scale and volume. $OPEX_y$ accounts for the maintenance costs of the system (excluding the fuel-fired generator) and $C_y^{a,M}$ of all components of the system and the fuel costs C_t^D of the generator. The maintenance costs C_t^{DM} of the generator depends upon its actual unit commitment, as described in (4). The fuel costs C_t^D detailed in (5) are modelled by using a piece-wise linear cost function. The load curtailment costs are proportional to the curtailed energy, as shown in (6).

$$NPC = CAPEX + \sum_{y \in Y} \frac{OPEX_y + REP_y + RES_y}{(1+d)^y} \tag{1}$$

$$CAPEX = \sum_{a \in A} C_0^a \left(\frac{X^a}{x_0^a} \right)^{\beta^a} \tag{2}$$

$$OPEX_y = \sum_{a \in A/\{D\}} C_y^{a,M} + \sum_{t \in T} C_t^D + C_t^{D,M} + C_t^{LC} \tag{3}$$

$$C_t^M = c^{D,M} X_t^D \tag{4}$$

$$C_t^D \geq \pi^F \left(c_i^{D,I} X^D + c_i^{D,S} P_t^D \right) \qquad \forall i \tag{5}$$

$$C_t^{LC} = c^{LC} P_t^{LC} \tag{6}$$

The AC and DC electrical balance are guaranteed by (7) and (8), respectively. P_t^D is the dispatch of the fuel-fired generator, $P_t^{I+/-}$ represents the power supplied by the inverter, P_t^{RAC} is the actual renewable production injected on the AC busbar (i.e. wind or hydro), P_t^L denotes the load demand and P_t^{LC} is the load curtailment. The DC balance expressed by equation (8) accounts for the power P_t^{RDC} produced by the renewable assets connected at the DC busbar, the output of the battery $P_t^{B+/-}$ and the one of the inverter, including its efficiency η^I.

$$P_t^D + P_t^{I+} - P_t^{I-} + P_t^{RAC} = P_t^L - P_t^{LC} \tag{7}$$

$$P_t^{RDC} + P_t^{B+} - P_t^{B-} - \frac{P_t^{I+}}{\eta^I} + P_t^{I-} \eta^I = 0 \tag{8}$$

The simulation tool is developed to guarantee the adequacy of the size of the components of the system, as detailed in (9)-(13). Variables x represents the size of the different components: generator (D), battery converter (C), inverter (I) and renewable assets, be them connected at the AC busbar (RAC) or DC one (RDC). The dispatching of the fuel generator takes into account the presence of the technical minimum, when the generator is turned on. Parameters $p_t^{RAC/RDC}$ denote the specific renewable production for unit size of the corresponding asset.

$$\alpha^{D,min} X^D Z_t^D \leq P_t^D \leq X^D Z_t^D \tag{9}$$

$$P_t^{B+} + P_t^{B-} \leq X^C \tag{10}$$

$$P_t^{I+} + P_t^{I-} \leq X^I \tag{11}$$

$$P_t^{RAC} \leq p_t^{RAC} X^{RAC} \tag{12}$$

$$P_t^{RDC} \leq p_t^{RDC} X^{RDC} \tag{13}$$

The energy balance of the battery is modelled by (14), in which E_t^B represents the energy available in the battery and η^B is its roundtrip efficiency, including the efficiency of the battery converter. The minimum and maximum state of charge of the battery are guaranteed by equation (15).

$$E_t^B = E_{t-1}^B - \frac{P_t^{B+}}{\sqrt{\eta^B}} + P_t^{B-}\sqrt{\eta^B} \tag{14}$$

$$\alpha^{B,min} X^B \leq E_t^B \leq \alpha^{B,max} X^B \tag{15}$$

According to LFS [18], the battery keeps the system in balance when a mismatch between actual energy production and load demand occurs. When the battery cannot meet the entire demand and the cost of curtailment would be higher than turning on the generator, the genset kicks in to fill the gap. The generator is kept off otherwise.

3. The multi-objective methodology

The proposed MDO-MOPSO procedure, shown in Fig. 2, is based on a modified version of the MOPSO algorithm [47]. In this activity, the classical version of the MOPSO method, based on [48] and [49], is further enhanced (1) by including the storage of all partial results simulated in the optimization process, (2) by improving the convergence metrics, accounting for spread and crowding distances [50, 51] similarly to NSGA-II [52] and DMS [51], and (3) by including a post-processing methodology aimed to identify the desired MDOs. Converesely to [51], a quadratic distance measure has been used; more details about the procedure are discussed as follows. Being recognized as key criteria for business investors [18], the objective functions considered in this activity are NPC and CAPEX; the optimization variables are the size of the main components of the system (Fig. 1).

The MDO-MOPSO algorithm is released at [53] for public use.

3.1. The optimization algorithm

The core of the proposed MDO-MOPSO procedure, shown in Fig. 2, is a modified version of the MOPSO algorithm [49], which is the multi-objective version of the traditional nature-inspired PSO heuristic algorithm that simulates the behavior of a number of organisms moving according to the local and global best positions that have been found at a given moment in the search-space [54]. Traditionally, the following steps are performed [49]:

1. Initialize the repository of the Pareto frontier and the working set of non-dominated size solutions, also referred to as particles, given the search area of the optimization variables.
2. Initialize the speed and position of each particle.
3. Iterate until convergence criteria are met:
    - 3.1. Update the speed and position of each particle in the working set.
    - 3.2. Apply mutation on particles to avoid falling in local optima.
    - 3.3. Evaluate the objectives for each particle (i.e. NPC and CAPEX).

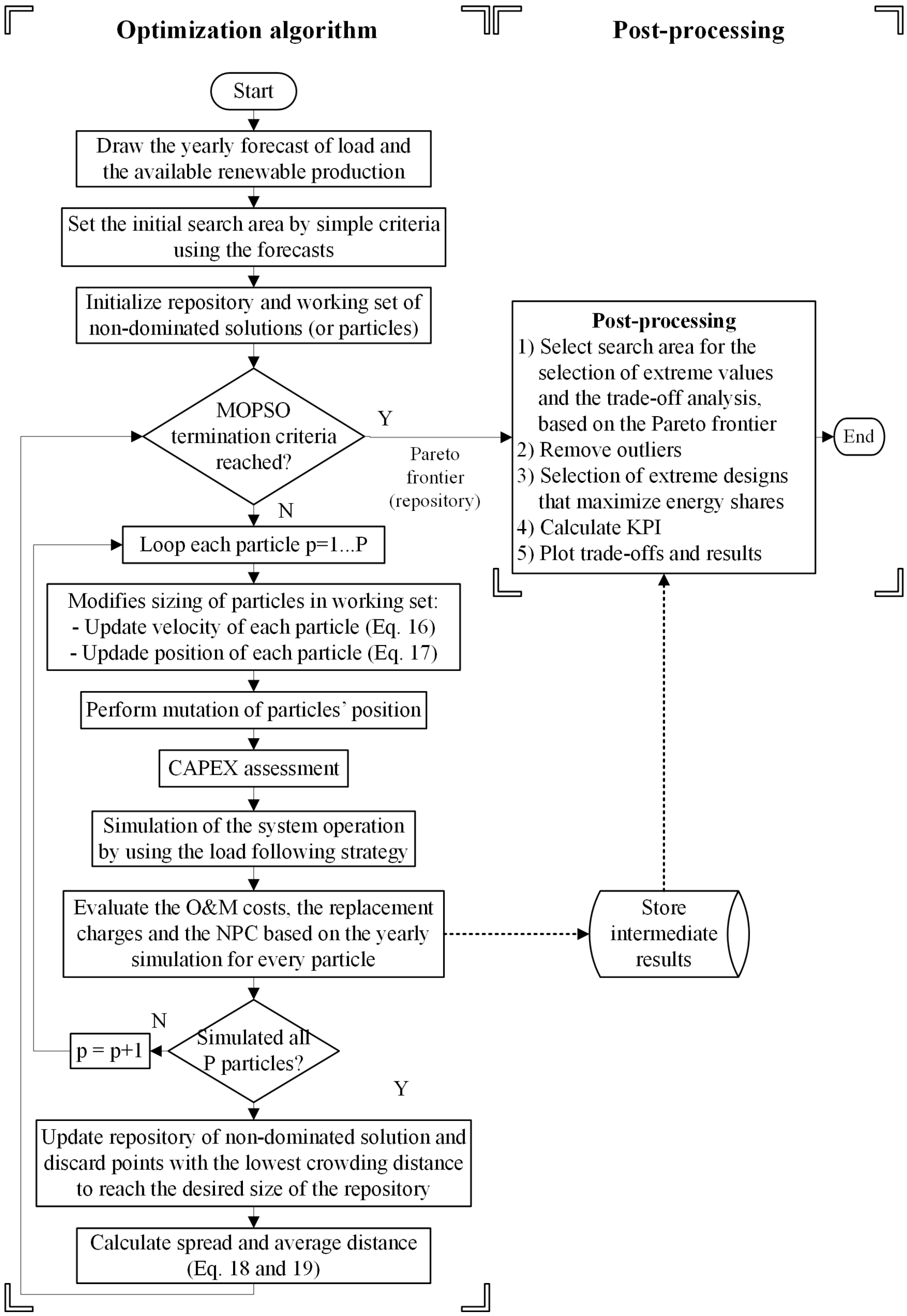

Figure 2: The proposed multi-objective MDO-MOPSO methodology.

3.4. Add non-dominated solutions to the repository.
3.5. When the repository is larger than the desired size of the Pareto frontier, remove points by using crowding distances.
3.6. Update convergence criteria (i.e. number of iterations).
4. The repository contains the desired Pareto frontier.

In the initialization phase, two sets, i.e. the working set and repository, are initialized by randomly sample the search space of the optimization variables (particles). The repository is used to store the updated Pareto frontier at each iteration, while the working set is used to explore the search space, that has to be provided to the algorithm. In this study, similarly to [34], the initial search area is calculated by using simple criteria based on the forecasts of the load and renewable sources; for example: the peak power of the inverter shall be equal to the peak power of the demand and the size of the battery shall be proportional to the daily demand, eventually including a confidence factor (i.e. 30% higher).

Each particle i is represented as a numeric vector whose speed $V_{i,t}$ and position $X_{i,t}$ is updated at each iteration t, according to equations (16) and (17), where $X_{i,t}^{P,best}$ is the best position of the particle found till the current iteration, $X_t^{G,best}$ is the non-dominated point corresponding to the current particle, parameters c_1 and c_2 are social constants modelling the personal and swarm confidence, and w represents the inertia of the system [47]. Quantities $r_{A/B,t}$ are random values extracted with uniform probability in the interval between 0 and 1.

A mutation process occurs in the dataset to avoid the optimizer to stuck in local optima [47, 49]. The dataset is divided in three categories that are modified with different rules: the first is not changed, the second one is subject to a uniform mutation and the third one to a non-uniform mutation.

$$\begin{aligned} V_{i,t+1} = wV_{i,t} + c_1 r_{A,t} \left(X_{i,t}^{P,best} - X_{i,t} \right) \\ + c_2 r_{B,t} \left(X_t^{G,best} - X_{i,t} \right) \end{aligned} \tag{16}$$

$$X_{i,t+1} = X_{i,t} + V_{I,t+1} \tag{17}$$

After the mutation phase, the algorithm simulates the microgrid operation for the entire optimization period (one year) and calculates the correspondent objective functions (Net Present Cost and CAPEX). It is worth noticing that selected data are stored after every simulation so that they can be post-processed when the multi-objective procedure is finished. In particular, conversely to the standard MOPSO methodologies [47, 49, 36, 37, 40, 38, 39], in this activity all the intermediate solutions are stored, as shown in Fig. 2.

When all the particles have been simulated, the repository of the points of the Pareto frontier is updated. Only the points with higher crowding distance are kept [47], as done in many multi-objective approaches such as Non-dominated Sorting Genetic Algorithm (NSGA-II) [55].

Then, the convergence criteria are calculated. Conversely to [47, 49], in which only the number of iterations is considered, in this activity we introduced the spread and the mean of the crowding distances as convergence criteria, which are used in NSGA-II [52] and DMS [51] algorithms. Furthermore, conversely to [51], in this activity we considered the quadratic mean instead of the average, to improve the quality of the frontier. The mathematical expression of the spread is reported in (18), where μ quantifies if the extreme values of the Pareto frontier have changed in two consecutive iterations, σ and $\bar{d}$ are the standard deviation and arithmetical average of the crowding distances, and Q is the number of points. The quadratic mean is instead calculated as in (19).

$$spread = \frac{\mu + \sigma}{\mu + Q\bar{d}} \tag{18}$$

$$quad\ mean = \sqrt{\frac{1}{Q}\sum_{k} d_k^2} \tag{19}$$

Finally, iterations stop when one of the following three criteria is met: (1) maximum number of iterations (100), (2) change of spread measure below a given relative and absolute tolerance (10^{-5}) [50, 55] or (3) change of the quadratic mean of the crowding distances below a given absolute and relative tolerance [50, 51].

The MATLAB code of the MDO-MOPSO algorithm used in this activity can be found at [53].

3.2. The post-processing

In the post-processing phase, all the designs simulated in the modified MOPSO algorithm are analyzed along with the final Pareto frontier. In particular, the targets of this analysis are: (1) selecting a limited set of multiple design options for developers to highlight different sizing characteristics w.r.t. the points in the Pareto frontier, but very close in terms of objective functions, (2) highlighting the trade-off of installing the different components, as delimited by a tolerance around the objective function values, and (3) comparing the two sets by using the selected KPIs. The approach is detailed below.

1. Given the Pareto frontier of the objective functions, the developer specifies the portion of the curve most suited for its technical and non-technical (i.e. financial) circumstances of the specific project. We recommend to focus on points nearby the Pareto frontier, e.g. within 3% of optimality, eventually restricting further the extrema of the analysis, for instance imposing limits on the other objective functions, such as CAPEX, to identify MDOs. Furthermore, within this area, the developer can specify narrower ranges around the objective function values to evaluate the relationship among the sizing of the components in the nearby of the same point of the Pareto frontier.
2. Outliers, such as size configurations that include a battery but not its converter or vice versa, are removed from the analysis.
3. Among the remaining points, the so-called "extreme designs" are selected that maximize or minimize energy shares or the size of components; we

mean, in particular, the largest and the lowest shares of AC and DC renewable production, as well as the minimum values of fuel-based generation, Energy-Not-Served (ENS), CAPEX and NPC. These points are the MDOs proposed to the developer and complement the options provided by the Pareto frontier.

4. Evaluation of the KPIs in the specified region, based on Manhattan measure [56], to compare the diversity characteristics of the original Pareto frontier and of the enhanced set of the Pareto frontier including the MDO points, as more detailed below.
5. Finally, the results are shown in plots and tables and compared to the traditional Pareto frontier.

Several dissimilarities measures are used in the literature [56] and are here adapted to compare the design characteristics (PV, wind, and battery design, and diesel production share) of the Pareto points, traditionally calculated in multi-objective optimization, and the enhanced set including the Pareto points and the MDOs, performed in the proposed procedure. The Manhattan measure has been selected because it is sensitive to outliers and easy to appraise, given its simplicity, with respect to other common metrics, such as cosine distance [56]. The mathematical representation to calculate the proposed diversity index ($DI^A(P)$) between points of a set P is detailed in (20), where $di(p, Q)$ quantifies the normalized diversity between a point p and any point q of set Q based on Manhattan distance, as detailed in (21); p_i and q_i represent the component i of points p and q, respectively. Moreover, it is useful also to define the same KPI to evaluate the diversity index between two different sets (P and Q) of points, as detailed in (22). Finally, in order to better compare KPIs corresponding to sets of different sizes, the normalized KPIs are defined as the absolute values over the size of the set under consideration, as specified in (23) and (24).

$$DI^A(P) = \sum_{p \in P} di(p, P/p) \tag{20}$$

$$di(p, Q) = \min_{q \in Q} \sum_{i} \frac{|p_i - q_i|}{|q_i|} \tag{21}$$

$$DI^A(P, Q) = \sum_{p \in P} di(p, Q/p) \tag{22}$$

$$DI^N(P) = \frac{DI^A(P)}{|P|} \tag{23}$$

$$DI^N(P, Q) = \frac{DI^A(P, Q)}{|P|} \tag{24}$$

4. Case study

4.1. Contextualization

The methodology discussed in the previous section has been applied to a case study for a real microgrid in Habaswein, located in a desert area in Eastern Kenya [34]; given the hybridization process ongoing in Kenyan microgrids [57], this case study can be representative of several contexts in the region. Real demand data have been collected and transcribed from the field for the 2014 at 30-min resolution and here averaged for every hour. At the time of measurement, the number of connections was around 2,000, for a total yearly demand of about 1.1 GWh and a peak power below 300 kW. Due to the location of the site, the main renewable sources are solar and wind, while no hydro source is available. Currently, the microgrid could potentially enlarge the existing PV and wind power plants, whose capacity factors are 20.8% and 31.2%, respectively, as estimated with the methodology in [58].

In the proposed case study, the PV installation is connected to the DC busbar, while the wind turbine supplies AC power. A lithium battery storage is also coupled to the DC busbar through a converter, and a backup diesel generator is also considered. The topology of the system is the same as depicted in Fig. 1.

4.2. Test description

The proposed methodology (Fig. 2) has been applied to the previously described microgrid. The decision variables are the capacities of the PV plant, wind farm, battery storage, battery converter, inverter, and diesel generator. First, the multi-objective optimization algorithm is run, while each sub-optimal solution is stored. All stored points that are within 3% of optimality of the Pareto frontier are then selected for post-processing, based on the findings of [7]; however, a sensitivity analysis is also performed to highlight the size of the selected points as a function of the optimality tolerance. As developers are interested in reducing both the total project costs (NPC) and the initial investment (CAPEX), it is expected that they would choose a design that is a compromise between the two economic indicator. In this analysis, for instance, the post-processing analysis narrows down to those solutions whose CAPEX is between 1 M$ and 1.25 M$, and the corresponding NPC is around 2.5M$. This range is considered as reasonable for this specific project after consulting with in-field experts given the partial obtained results (the maximum CAPEX is up to 1.5M$). In fact, high CAPEX investments expose the company to higher risks and lower profit-to-investment ratio, as confirmed by the multi-objective approach developed in [18], yet without a MDO methodology; thus investments in rural electrification projects are often a compromise between the size of the initial investment and the profitability of the specific project. Finally, in order to examine the variation in size of the components nearby the Pareto frontier, an extra analysis has been made on the points at three pre-determinated CAPEX location (0.5, 0.9 and 1.2 M$) plus a $\pm 20k\$$ tolerance. Again, these three locations have been proposed as representative of a suitable range for typical microgrid investments, in order to highlight the consistency of the results along the Pareto frontier.

4.3. Inputs

Table 1: Main parameters of the components.

Asset (a)	$S_{i,0}$; UM	$C_{i,0}$ [$/UM]	β_i [-]	Maintenance [$/UM/y]	Lifetime
PV	1 kW	900	1	10	25y
Wind	1 kW	4000	0.9	80	20y
Battery	1 kWh	750	0.9	3	3000 e.c.*
Bat. conv.	1 kW	1258	0.5	2	15y
Inverter	1 kW	1887	0.5	2	15y
Fuel gen.	1 kW	1000	0.8	0.05$/kW/h	30000h

*Equivalent full cycles at 80% Depth of Discharge

The main economic and technical parameters of the microgrid components are detailed in Table 1. The roundtrip efficiency of the battery including the battery converter is 94%, while the one of the inverter is 96%. The efficiency of the diesel generator is modelled with a piece-wise linear function whose maximum efficiency is 33% at rated power and the minimum working point is 10%. The load curtailment cost is 2$/kWh and the fuel price is 0.9$/l. The battery is operated between 20% and 80% of state of charge so that its lifetime amounts to 3,000 equivalent full cycles. The discount rate is 8% and the lifetime of the project is 20 years. The optimizations have been performed at hourly time steps on a 6-core computer with 16 GB RAM and completed in about 3 minutes.

5. Results

Selected results are shown in Fig. 3, Fig. 4, Fig. 5, Fig. 6, Table 2, Table 3 and Table 4. Fig. 3 reports the Pareto frontier in red, while the sub-optimal points within 3% tolerance from the frontier are shown in blue. Their generation share that corresponds to each of these points is plotted in Fig. 4. Fig. 5 details the size configurations of those solutions in the Pareto frontier and the results obtained from the post-processing phase. The corresponding numerical results are detailed in Table 2 and Table 3. Fig. 6 depicts the additional analyses applied to the points of the areas A, B and C, as defined in Section 4.2 and highlighted in Fig. 3. Finally, the results of the KPI analysis are reported in Table 4, while the sensitivity with respect to the number of selected points is reported in Table 5.

5.1. Analysis of the Pareto frontier

The frontier depicted in Fig. 3 clearly shows that when the initial investment is too limited (i.e. below 50 k$) the NPC is significantly high, even beyond 5-10 M$, due to paramount load curtailment costs. In contrast, increasing the CAPEX from 60 k$ up to 1.6M$ only halves the NPC. This suggests that each single optimization (minimizing NPC or CAPEX) would result in extreme solutions, while a developer would rather choose a point in between so to comply with the available funding for the initial investment and incur in reasonable long-term costs.

As CAPEX increases, more renewable assets are installed and the energy share changes from strictly relying on diesel production (with large values of ENS when the installed capacity is not enough to meet the load) to an increasing renewable penetration, as shown in Fig. 4. However, it is worth noticing that trends are not linear and that the points within 3% tolerance provide large variations in the sizes and in the corresponding energy shares of each component with respect to the closest point in the Paretor frontier. Most of the variation and noise are related to PV and wind sizing. Nevertheless, variations of about 10% in share between renewable sources and diesel production also occur. This suggests that multiple design solutions may correspond to similar values of CAPEX and NPC, despite having significant different characteristics in terms of components. All this confirms the rationality of the proposed methodology and the practical outcomes of this study. Hence, the need for a methodology as the one proposed in this paper, which is our major contribution.

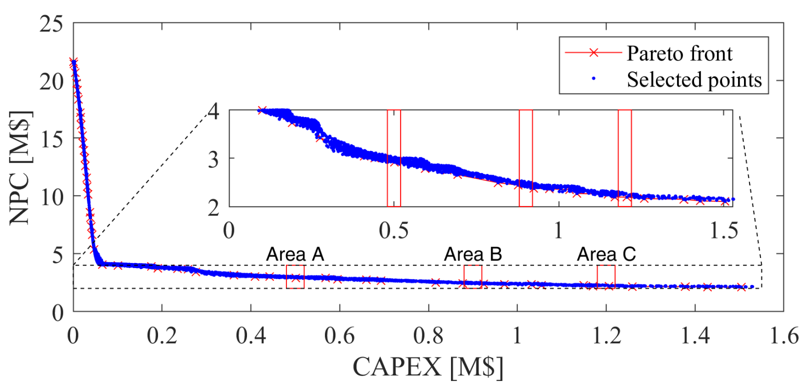

Figure 3: The Pareto frontier: the red dots define the Pareto frontier, while the blue points are within 3% tolerance.

5.2. Selection of extrema points

The points selected by the post-processing as described in Section 3.2 are shown in Fig. 5 in green. Table 2 details the economics and energy share for each selection criteria and their numerical values, while Table 3 reports the optimal

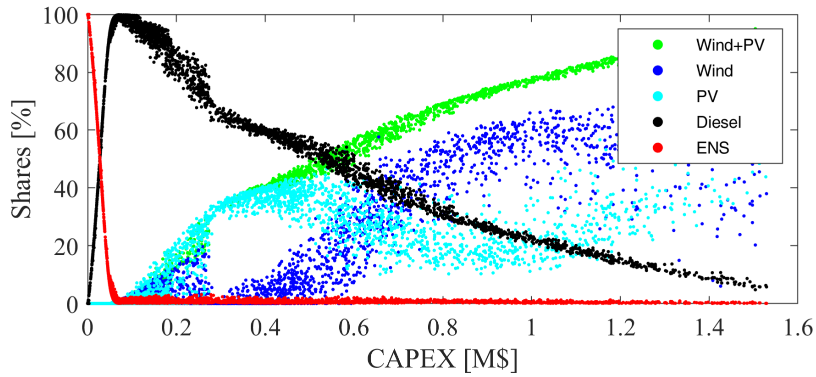

Figure 4: Production share; all points are within 3% tolerance of the Pareto frontier.

sizing. The red dots in Fig. 5 show the Pareto frontier and the rest of the points are within 3% optimality.

The results in Fig. 5 highlight that the Pareto frontier of the traditional multi-objective approach does not guarantee to capture all the interesting size solutions close to the Pareto frontier itself. In fact, the points within 3% optimality in Fig. 5 span a very large range of values, while the Pareto frontier (in red dots) has a rather smooth behavior that does not capture the scattering of the other points, which instead can be performed by the proposed approach that has selected the MDO points shown in green.

Fig. 5 shows that the size of the components, even when close to the Pareto frontier (hence with similar values of objective functions), can exhibit variations of up to 100% with respect to the ones placed on the Pareto frontier. For example, as detailed in Table 2, the solutions minimizing ENS and maximizing the share of the PV plant are quite close in terms of objective function, but differ by 24-25% in terms of energy shares of PV and wind sources and ENS in the latter is about 7 times higher. The design minimizing CAPEX is close to the one minimizing the PV share, but in the latter wind share is 10% higher than in the former. Likewise, the design minimizing ENS is very close to the Pareto frontier (points 3), however the ENS is halved in the MDO solution. The solution with the highest PV production is comparable with point 3 of the Pareto frontier, but the corresponding PV production is 20% higher. Therefore, these results confirm that our approach successfully provides multiple design options with characteristics significantly different with respect to the optimal Pareto solutions, without deteriorating the economics of the project. Similar considerations can be performed on the final optimal design of the points belonging to the Pareto frontier and the selected MDOs, as detailed in Table 3. These findings confirm the rationality of the proposed approach and the ability of the proposed approach to help developers in tackling externalities that can hardly be computed in the objective functions.

Fig. 5d shows that the sizing of the diesel generator is slightly affected by

CAPEX, since it is relatively cheap to install the generator. However its dispatching is significantly affected, given the results of Fig. 4. On the other side, due to their high investment costs, renewable sources become profitable beyond 100-400 k$ CAPEX, as highlighted in Fig. 5a and Fig. 5b, whereas batteries are installed only beyond 600-800k$ CAPEX (Fig. 5c). In particular, the general trend in the installation of such components exhibits a significant non-linear behavior, mainly due to their investment costs and the correlation between the renewable production and load, as well as the rest of parameters. In fact, the equivalent LCOE of the PV production is lower than wind, which is the reason why PV is installed at lower CAPEX than wind. However, as the PV production is available only during the day, it is also worthy to install wind turbines later. Lastly, for higher values of CAPEX, it is profitable to install batteries and defer the electricity produced by the two renewable sources. This effect is especially observable for the PV one, as suggested by the large increase in the PV share as long as batteries are installed. It is worth noticing that as more batteries are installed, PV source is more likely to be included over wind because the specific production cost of the former is lower.

Table 2: Economics and energy share of the extreme points selected by the procedure and points belonging to the Pareto frontier.

Criterion	Economics NPC [M$]	Economics CAPEX [M$]	Shares PV [%]	Shares Wind [%]	Shares Diesel [%]	Shares ENS [%]
min CAPEX	2.31	1.00	21.1	57.1	21.4	0.37
min PV	2.42	1.04	12.0	66.8	20.4	0.82
min ENS	2.29	1.14	32.3	50.1	17.6	0.07
max PV/min Wind	2.28	1.15	56.6	25.8	17.0	0.50
max Wind	2.29	1.18	15.7	68.0	16.0	0.35
min Diesel	2.21	1.24	42.7	44.3	12.5	0.55
min NPC	2.18	1.24	35.4	51.4	12.9	0.21
Pareto 1	2.35	1.03	18.4	60.0	21.4	0.23
Pareto 2	2.27	1.05	21.6	58.6	19.6	0.23
Pareto 3	2.25	1.15	39.0	43.9	17.0	0.15
Pareto 4	2.20	1.17	36.7	48.0	14.8	0.49
Pareto 5	2.19	1.21	46.5	39.2	13.9	0.38

5.3. Trade-off analysis

The three plots reported in Fig. 6 zoom into the points belonging to areas A, B and C of Fig. 3. First of all, it is worth noticing that each area (A-C) groups a consistent number of possible designs with similar profitability, as they are selected according to the small CAPEX and NPC tolerances previously discussed; at the same time, as shown in Fig. 4 and Fig. 5, the sizes and energy shares corresponding to the different points are significantly different. Indeed, the aim of Fig. 6 is to specifically highlight the correlations among the design

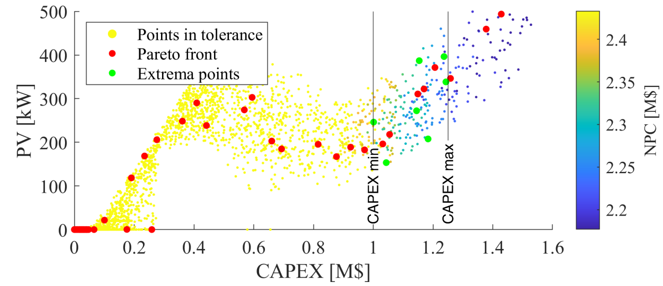

(a) Size of the PV plant

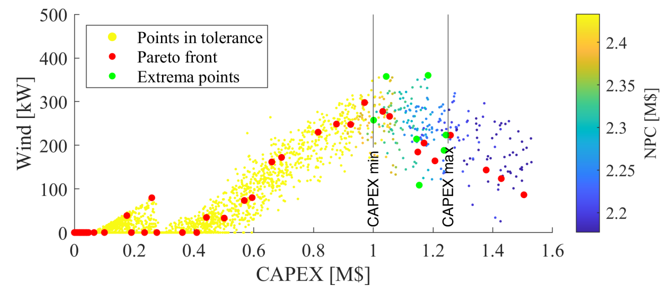

(b) Size of the wind farm

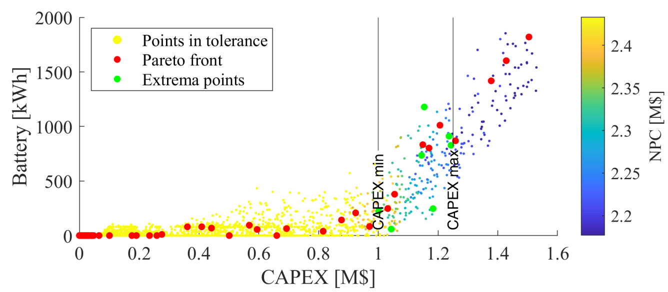

(c) Size of the battery bank

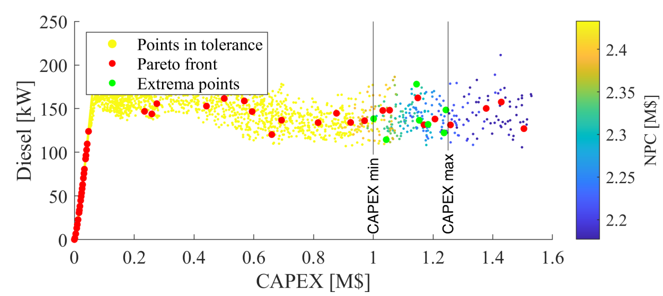

(d) Size of the diesel generator

Figure 5: Design of the system: the red dots represent the Pareto front, the green ones are the extreme points selected according to the post-processing approach and the remaining are the points within 3% tolerance w.r.t. the Pareto front.

Table 3: Design of the extreme points selected by the procedure and points belonging to the Pareto frontier.

Criterion	Design PV [kW]	Wind [kW]	Battery [kWh]	DCDC [kW]	Inv [kW]	Diesel [kW]
min CAPEX	246	258	223	108	187	138
min PV	153	358	59	140	133	114
min ENS	272	214	735	151	339	178
max PV/min Wind	387	109	1179	309	168	137
max Wind	208	360	247	111	202	132
min Diesel	396	188	911	131	202	122
min NPC	338	224	828	168	249	149
Pareto 1	196	278	248	415	346	148
Pareto 2	218	266	379	131	150	148
Pareto 3	311	185	833	155	400	162
Pareto 4	322	205	802	152	168	132
Pareto 5	371	164	1012	243	198	138

or production shares of different assets, according to the following scheme: the size of the and of the wind farm are on the X- and Y-axis, respectively, while the energy capacity of the storage and the diesel production share are indicated by the color and the size of the dot, respectively. It is worth noticing that in the proposed analysis we didn't consider the size of the diesel generator because it is only slightly affected by the sizing of the other assets, as shown in Fig. 5d; rather, we focused on the production share of the fuel generator, which is more affected as depicted in Fig. 6.

The pictures show a clear trade-off between the design of PV and wind assets: the larger the PV plant, the smaller the wind farm for a similar value of the objective functions. It is worth noticing that the slope between the size of the wind farm and the PV plant reflects the corresponding ratio of the LCOE, which is around 0.41-0.48 including economies of scale in the range of interest (50-400 kWp of wind farm); in fact, the results suggest that every kWp of PV plant could be generally replaced by about 0.4-0.43kW of wind turbine, depending on the size of the wind turbine. Instead, when CAPEX are limited and the size of batteries is not significant (Fig. 6a), the substitution ratio falls below 0.4 and exhibits a non-linear behavior, also due to the contemporaneity between the load profiles and the specific renewable production.

Similarly, the higher the size of the batteries, the lower the sizes of the PV and wind plants, especially in Fig. 6b and Fig. 6c where batteries become economically profitable given the corresponding level of CAPEX. Instead, when CAPEX are low (Fig. 6a), the design of the system rarely includes batteries.

As in Fig. 6a, the use of the generator tends to increase when a renewable source is predominant over the other and the battery capacity is small, while the fossil production tends to decrease when the contribution of the two renewable

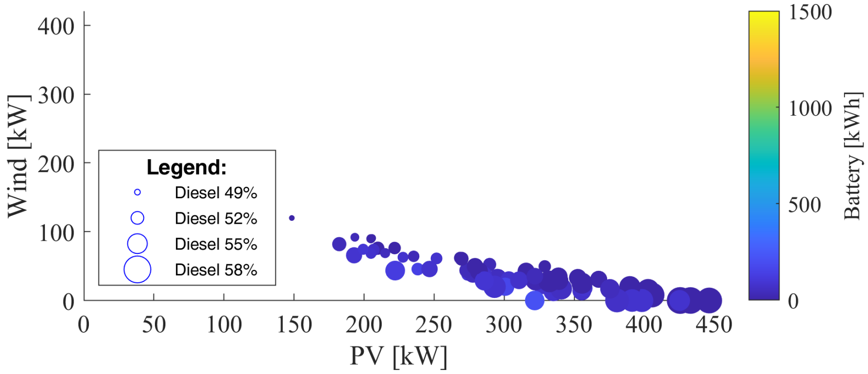

(a) Area A

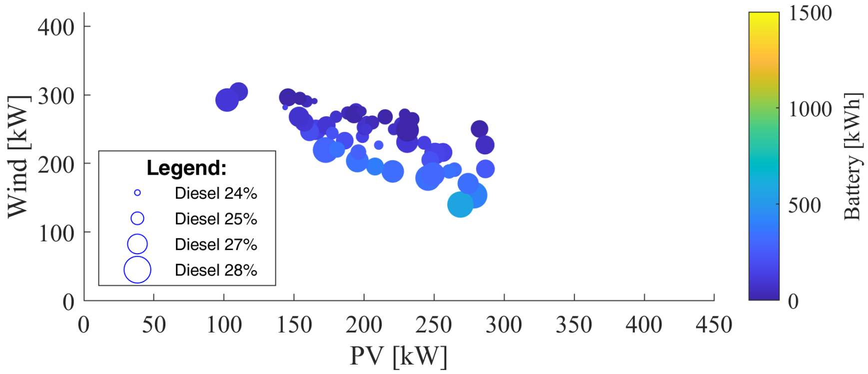

(b) Area B

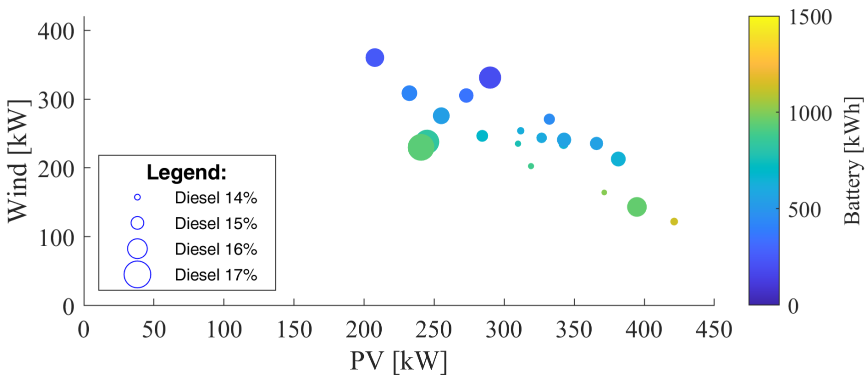

(c) Area C

Figure 6: Trade-off between the installation of the main components of the system for the points in the trade-off areas A, B and C.

sources is more balanced. In cases B and C (Fig. 6b and Fig. 6c), the production share between the sources is more balanced and storage is often included, thus the diesel production changes only by 3-4%, while in Fig. 6a the difference is larger. These analyses can be very interesting for the planning phase of microgrid projects and can help developers to meet the multifaceted and peculiar circumstances of the specific business environment in which they are playing.

5.4. KPI analysis

Table 4 highlights the value of the KPI defined in Section 3.2 when applied to the set of the MDO points and on points (set S^{PF}) belonging to the Pareto Frontier in the selected region; while the first row highlights the absolute value of the KPI, the second row states the specific KPI per point of the set under consideration. The objective of this normalization is to compare sets with different size.

Table 4: Absolute and normalized KPIs.

	$DI(S^{PF})$	$DI(S^{PF} \cup S^{MDO})$	$DI(S^{MDO}, S^{PF})$
Abs. KPI DI^A [-]	0.667	1.614	1.067
Norm. KPI DI^N [-]	0.133	0.135	0.152

The proposed approach successfully selects points far from the Pareto frontier; in fact, the absolute KPI with the proposed approach ($DI^A(S^{PF} \cup S^{MDO})$) is almost three times the value with the Pareto frontier only ($DI^A(S^{PF})$), as shown in the first row of Table 4. The reason is that the selected MDOs are significantly far from the Pareto frontier, as confirmed by the index $DI^A(S^{MDO}, S^{PF})$ that quantifies the diversity between sets S^{MDO} and S^{PF}.

The robustness of the proposed approach for this case study is further confirmed by the normalized KPI with respect to the size of the set under consideration, shown in the second row of Table 4. In fact, the normalized KPIs corresponding to the proposed approach (both $DI^N(S^{PF} \cup S^{MDO})$ and $DI^N(S^{MDO}, S^{PF})$) are never lower than in the Pareto frontier case ($DI^N(S^{PF})$), which means that not only the same specific diversity has been preserved, but it is even increased. It is worth noticing that since set $S^{PF} \cup S^{MDO}$ is composed by a larger set of points (12), while S^{PF} and S^{MDO} amount for 5 and 7, respectively, the corresponding absolute KPI ($DI^A(S^{PF} \cup S^{MDO})$) is likely to be higher; however, thanks to the proposed procedure, the selected MDOs are so distant that even the normalized KPI with MDO is higher than the one performed on the Pareto frontier only. In particular, the normalized diversity index ($DI^N(S^{MDO}, S^{PF})$) of MDOs is significantly higher than S^{PF}, calculated on the Pareto frontier set, which confirms that the proposed approach is able to select adequate different options with respect to the Pareto frontier.

5.5. Sensitivity on the optimality tolerance

In Table 5, we finally show the impact of the optimality tolerance on the number of points, outliers excluded, selected within the CAPEX range, with the goal of justifying the choice of the 3%-tolerance and to show the flexibility of the approach in identifying multiple possible designs. The results are organized by CAPEX range because the population of points may differ depending on the area of the Pareto frontier. The proposed visualization suggests that a tolerance of 3% is an adequate value to select a large number of possible different options, without compromising too much the optimality of the results. In fact, at 1% tolerance, few points are selected beyond 0.6-0.9M$ of investment; with a tolerance of 5%, or larger, the points selected by the procedure may be too sub-optimal and hence not attractive for the private developer.

Table 5: Number of size configurations selected in the different CAPEX ranges, as a function of the optimality tolerance, outliers excluded.

CAPEX range [M$]	Optimality tolerance [%]			
	1	3	5	10
≤0.3	829	1164	1518	2270
0.3-0.6	223	408	544	937
0.6-0.9	81	295	515	1057
0.9-1.2	63	243	425	848
≥1.2	27	109	237	639

6. Conclusions

The described methodology introduces the concept of multiple design options for hybrid microgrids with the aim of enhancing the planning capabilities of developers who are commonly confronting a multi-faceted business environment that cannot always inputted in optimization models, such as the maintenance complexity, uncertainties in the supply chain, or the availability of local skills. Conversely to traditional multi-objective approaches that calculate only the Pareto frontier, the proposed methodology is able to track multiple solutions, nearby the frontier, that have significantly different characteristics in terms of technology generation and size of components, so that developers can be provided with a larger number of options to meet the specific requirements of their investment. Our enhanced multi-objective approach iteratively simulates many size scenarios and stores the results that are subsequently post-processed. The final outcome is the identification of design scenarios that exhibit desired techno-economic features different from the Pareto solutions, without significantly affecting the economics of the project.

The results highlighted in this study confirm that many configurations with different proportion of installed assets can lead to economic results very similar to the Pareto ones, sometimes even excluding some particular asset from the design (hence differences of up to 100% in terms of sizing). This implies that the developer has access to multiple designs that can better meet the specific circumstances of the project even when these cannot be mathematically included in the optimization model. In fact, traditional mathematical methods have usually disregarded solutions that are slightly sub-optimal even for negligible amounts, which, however, may be preferable for the developers. The proposed KPI analysis confirms the validity of our approach.

This study lays the foundations for the development and improvement of several commercial tools for microgrid developments and can be easily extended to other research fields, such as for the optimal design of multi-source systems, eventually including thermal or mass storage, network investment decisions, or any system in which the same requirement can be met with different types of assets.

References

[1] IRENA International Renewable Energy Agency, Policies and regulations for renowable energy mini-grids, 2018.

[2] A. Kumar, B. Sah, A. R. Singh, Y. Deng, X. He, P. Kumar, R. C. Bansal, A review of multi criteria decision making (MCDM) towards sustainable renewable energy development, Renewable and Sustainable Energy Reviews 69 (2017) 596–609.

[3] H. M. Ridha, C. Gomes, H. Hizam, M. Ahmadipour, A. A. Heidari, H. Chen, Multi-objective optimization and multi-criteria decision-making methods for optimal design of standalone photovoltaic system: A comprehensive review, Renewable and Sustainable Energy Reviews 135 (2021) 110202.

[4] M. T. M. Emmerich, A. H. Deutz, A tutorial on multiobjective optimization: fundamentals and evolutionary methods, Natural Computing 17 (3) (2018) 585–609.

[5] Q. Liu, X. Li, H. Liu, Z. Guo, Multi-objective metaheuristics for discrete optimization problems: A review of the state-of-the-art, Applied Soft Computing 93 (2020) 106382.

[6] R. Khezri, A. Mahmoudi, Review on the state-of-the-art multi-objective optimisation of hybrid standalone/grid-connected energy systems, IET Generation, Transmission & Distribution 14 (20) (2020) 4285–4300.

[7] D. Fioriti, G. Lutzemberger, D. Poli, P. Duenas-Martinez, A. Micangeli, Heuristic approaches to size microgrids: a methodology to compile multiple design options, in: 20h IEEE Int. Conf. on Environ. and Electrical Engineering (EEEIC), IEEE, 2020, pp. 1–6.

[8] R. Siddaiah, R. P. Saini, A review on planning, configurations, modeling and optimization techniques of hybrid renewable energy systems for off grid applications, Renewable and Sustainable Energy Reviews 58 (2016) 376–396.

[9] J. Lian, Y. Zhang, C. Ma, Y. Yang, E. Chaima, A review on recent sizing methodologies of hybrid renewable energy systems, Energy Conversion and Management 199 (2019) 112027.

[10] V. Oree, S. Z. Sayed Hassen, P. J. Fleming, A multi-objective framework for long-term generation expansion planning with variable renewables, Applied Energy 253 (2019) 113589.

[11] E. L. Eriksson, E. M. A. Gray, Optimization of renewable hybrid energy systems – A multi-objective approach, Renewable Energy (2019) 971–999.

[12] M. A. Cuesta, T. Castillo-Calzadilla, C. E. Borges, A critical analysis on hybrid renewable energy modeling tools: An emerging opportunity to include social indicators to optimise systems in small communities, Renewable and Sustainable Energy Reviews 122 (2020) 109691.

[13] M. Gharibi, A. Askarzadeh, Technical and economical bi-objective design of a grid-connected photovoltaic/diesel generator/fuel cell energy system, Sustainable Cities and Society 50 (2019) 101575.

[14] C. D. Rodríguez-Gallegos, D. Yang, O. Gandhi, M. Bieri, T. Reindl, S. K. Panda, A multi-objective and robust optimization approach for sizing and placement of PV and batteries in off-grid systems fully operated by diesel generators: An Indonesian case study, Energy 160 (2018) 410–429.

[15] P. Conti, G. Lutzemberger, E. Schito, D. Poli, D. Testi, Multi-Objective Optimization of Off-Grid Hybrid Renewable Energy Systems in Buildings with Prior Design-Variable Screening, Energies 15 (15).

[16] M. Rodrigues, L. Mendes, Mapping of the literature on social responsibility in the mining industry: A systematic literature review, Journal of Cleaner Production 181 (2018) 88–101.

[17] C. Carnevale, M. Mazzuca, S. Venturini, Corporate Social Reporting in European Banks: The Effects on a Firm's Market Value, Corporate Social Responsibility and Environmental Management 19 (3) (2012) 159–177.

[18] D. Fioriti, S. Pintus, G. Lutzemberger, D. Poli, Economic multi-objective approach to design off-grid microgrids: A support for business decision making, Renewable Energy 159 (2020) 693–704.

[19] IRENA, Renewable Power Generation Costs in 2017, Tech. rep. (2018).

[20] M. A. Hannan, M. Faisal, P. Jern Ker, R. A. Begum, Z. Y. Dong, C. Zhang, Review of optimal methods and algorithms for sizing energy storage systems to achieve decarbonization in microgrid applications, Renewable and Sustainable Energy Reviews 131 (2020) 110022.

[21] T. Tezer, R. Yaman, G. Yaman, Evaluation of approaches used for optimization of stand-alone hybrid renewable energy systems, Renew Sust Energ Rev 73 (2017) 840–853.

[22] N. Komendantova, A. Patt, L. Barras, A. Battaglini, Perception of risks in renewable energy projects: The case of concentrated solar power in North Africa, Energy Policy 40 (2012) 103–109.

[23] N. J. Williams, P. Jaramillo, J. Taneja, T. S. Ustun, Enabling private sector investment in microgrid-based rural electrification in developing countries: A review, Renewable and Sustainable Energy Reviews 52 (2015) 1268–1281.

[24] P. A. Trotter, M. C. McManus, R. Maconachie, Electricity planning and implementation in sub-Saharan Africa: A systematic review, Renewable and Sustainable Energy Reviews 74 (June 2016) (2017) 1189–1209.

[25] K. Gebrehiwot, M. A. H. Mondal, C. Ringler, A. G. Gebremeskel, Optimization and cost-benefit assessment of hybrid power systems for off-grid rural electrification in Ethiopia, Energy 177 (2019) 234–246.

[26] T. Ma, H. Yang, L. Lu, A feasibility study of a stand-alone hybrid solar–wind–battery system for a remote island, Applied Energy 121 (2014) 149–158.

[27] C. Xiao, D. Sutanto, K. M. Muttaqi, M. Zhang, A Judicious Decision-Making Approach for Power Dispatch in Smart Grid Using a Multiobjective Evolutionary Algorithm Based on Decomposition, IEEE Trans. Ind. Appl. 56 (2) (2020) 1918–1929.

[28] S. R. Ghatak, S. Sannigrahi, P. Acharjee, Multiobjective Framework for Optimal Integration of Solar Energy Source in Three-Phase Unbalanced Distribution Network, IEEE Transactions on Industry Applications 56 (3) (2020) 3068–3078.

[29] M. A. Ashraf, Z. Liu, A. Alizadeh, S. Nojavan, K. Jermsittiparsert, D. Zhang, Designing an optimized configuration for a hybrid PV/Diesel/Battery Energy System based on metaheuristics: A case study on Gobi Desert, Journal of Cleaner Production 270 (2020) 122467.

[30] M. Giuntoli, D. Poli, On the possible use of probabilistic techniques for purposes of short-term load dispatching, International Review of Electrical Engineering, IREE 8 (4) (2013) 1243–1252.

[31] Y. Liu, R. Sioshansi, A. J. Conejo, Multistage Stochastic Investment Planning With Multiscale Representation of Uncertainties and Decisions, IEEE Transactions on Power Systems 33 (1) (2018) 781–791.

[32] H. Khaloie, A. Abdollahi, M. Shafie-khah, A. Anvari-Moghaddam, S. Nojavan, P. Siano, J. P. Catalão, Coordinated wind-thermal-energy storage offering strategy in energy and spinning reserve markets using a multi-stage model, Applied Energy 259.

[33] V. Rasouli, I. Goncalves, C. H. Antunes, A. Gomes, A Comparison of MILP and Metaheuristic Approaches for Implementation of a Home Energy Management System under Dynamic Tariffs, SEST 2019 - 2nd Int Conf on Smart Energy Systems and Technologies.

[34] A. Micangeli, D. Fioriti, P. Cherubini, P. Duenas-martinez, Optimal Design of Isolated Mini-Grids with Deterministic Methods : Matching Predictive Operating Strategies with Low Computational Requirements, Energies 13.

[35] S. Mostaghim, J. Teich, Strategies for finding good local guides in multi-objective particle swarm optimization (MOPSO), in: Proceedings of the 2003 IEEE Swarm Intelligence Symposium. SIS'03 (Cat. No.03EX706), 2003, pp. 26–33.

[36] X. Xu, W. Hu, D. Cao, Q. Huang, C. Chen, Z. Chen, Optimized sizing of a standalone PV-wind-hydropower station with pumped-storage installation hybrid energy system, Renewable Energy 147 (2020) 1418–1431.

[37] M. Azaza, F. Wallin, Multi objective particle swarm optimization of hybrid micro-grid system: A case study in Sweden, Energy 123 (2017) 108–118.

[38] B. Lokeshgupta, S. Sivasubramani, Multi-objective dynamic economic and emission dispatch with demand side management, International Journal of Electrical Power & Energy Systems 97 (2018) 334–343.

[39] D. Suchitra, R. Jegatheesan, T. J. Deepika, Optimal design of hybrid power generation system and its integration in the distribution network, International Journal of Electrical Power & Energy Systems 82 (2016) 136–149.

[40] H. Borhanazad, S. Mekhilef, V. Gounder Ganapathy, M. Modiri-Delshad, A. Mirtaheri, Optimization of micro-grid system using MOPSO, Renewable Energy 71 (2014) 295–306.

[41] Y. Cao, Y. Zhang, H. Zhang, X. Shi, V. Terzija, Probabilistic Optimal PV Capacity Planning for Wind Farm Expansion Based on NASA Data, IEEE Transactions on Sustainable Energy 8 (3) (2017) 1291–1300.

[42] B. Wang, S. Wang, X. Zhou, J. Watada, Two-Stage Multi-Objective Unit Commitment Optimization Under Hybrid Uncertainties, IEEE Transactions on Power Systems 31 (3) (2016) 2266–2277.

[43] A. Zeinalzadeh, Y. Mohammadi, M. H. Moradi, Optimal multi objective placement and sizing of multiple DGs and shunt capacitor banks simultaneously considering load uncertainty via MOPSO approach, International Journal of Electrical Power and Energy Systems 67 (2015) 336–349.

[44] K. Anoune, M. Bouya, A. Astito, A. B. Abdellah, Sizing methods and optimization techniques for PV-wind based hybrid renewable energy system: A review, Renewable and Sustainable Energy Reviews 93 (2018) 652–673.

[45] A. Bosisio, M. Moncecchi, G. Cassetti, M. Merlo, Microgrid design and operation for sensible loads: Lacor hospital case study in Uganda, Sustainable Energy Technologies and Assessments 36 (2019) 100535.

[46] L. Moretti, M. Astolfi, C. Vergara, E. Macchi, J. I. Pérez-Arriaga, G. Manzolini, A design and dispatch optimization algorithm based on mixed integer linear programming for rural electrification, Applied Energy 233-234 (November 2018) (2019) 1104–1121.

[47] V. Martínez-Cagigal, Multi-Objective Particle Swarm Optimization (MOPSO) (2020).
URL `https://www.mathworks.com/matlabcentral/fileexchange/62074-multi-objective-particle-swarm-optimization-mopso`

[48] C. A. C. Coello, G. T. Pulido, M. S. Lechuga, Handling multiple objectives with particle swarm optimization, IEEE Transactions on Evolutionary Computation 8 (3) (2004) 256–279.

[49] M. R. Sierra, C. A. Coello Coello, Improving PSO-Based Multi-objective Optimization Using Crowding, Mutation and E-Dominance BT - Evolutionary Multi-Criterion Optimization, Springer Berlin Heidelberg, Berlin, Heidelberg, 2005, pp. 505–519.

[50] MathWorks, Multiobjective Optimization - MATLAB & Simulink.
URL `https://it.mathworks.com/help/gads/multiobjective-optimization.html`

[51] A. L. Custódio, J. F. Madeira, A. I. Vaz, L. N. Vicente, Direct multisearch for multiobjective optimization, SIAM Journal on Optimization 21 (3) (2011) 1109–1140.

[52] K. Deb, Multi-Objective Optimization Using Evolutionary Algorithms, Chichester, England, 2001.

[53] D. Fioriti, MDO - MOPSO (2020).
URL `https://www.mathworks.com/matlabcentral/fileexchange/82174-mdo-mopso`

[54] S. Wen, H. Lan, Q. Fu, D. C. Yu, L. Zhang, Economic Allocation for Energy Storage System Considering Wind Power Distribution, IEEE Transactions on Power Systems 30 (2) (2015) 644–652.

[55] A. H. Keshavarzzadeh, P. Ahmadi, Multi-objective techno-economic optimization of a solar based integrated energy system using various optimization methods, Energy Conversion and Management 196 (2019) 196–210.

[56] A. S. Shirkhorshidi, S. Aghabozorgi, T. Ying Wah, A Comparison study on similarity and dissimilarity measures in clustering continuous data, PLoS ONE 10 (12).

[57] Ministry of Energy, KENYA OFF-GRID SOLAR ACCESS PROJECT (K-OSAP) VULNERABLE and MARGINALIZED GROUPS FRAMEWORK, Tech. Rep. March (2017).

[58] S. Pfenninger, I. Staffell, Long-term patterns of European PV output using 30 years of validated hourly reanalysis and satellite data, Energy 114 (2016) 1251–1265.